7th Int. Conf. on Circulating Fluidized Beds,
Niagara Falls, Ontario, May 5-7, 2002, p. 717-724

A CIRCULATING FLUIDIZED BED COMBUSTOR SYSTEM WITH INHERENT CO_2 SEPARATION -APPLICATION OF CHEMICAL LOOPING COMBUSTION

Eva Johansson*, Anders Lyngfelt, Tobias Mattisson and Filip Johnsson
Dept of Energy Conversion, Chalmers University of Technology, Göteborg, Sweden

Abstract − Possible operational conditions of a conceptual design of a circulating fluidized bed for chemical looping combustion (CLC) were investigated. CLC is a method where a gaseous fuel is combusted with inherent separation of the greenhouse gas CO_2 from the flue gas. Oxygen is transferred from the combustion air to a gaseous fuel by means of metal oxide particles acting as oxygen carriers. A bubbling bed below the downcomer acts as a fuel reactor where oxygen is transferred from the metal oxide (Me_xO_y) to the fuel and the riser acts as the air reactor, where the previously reduced metal oxide (Me_xO_{y-1}) is oxidized by the oxygen in the air. Hence, the fuel and combustion air are not in direct contact.

A cold model of such a system was designed and operated according to scaling laws corresponding to an original 30 MW_{th} combustor design operating at 0.9 MPa with natural gas as the fuel and iron oxide as the oxygen carrier. A mapping of the range of operational conditions with respect to combinations of fluidization velocity in the air reactor, bed mass, and the net solids flux (G_s), from the air to the fuel reactor is presented.

Introduction

It is generally accepted that the effect of global warming caused by emissions of greenhouse gases requires substantial measures in the near future in order to stabilize the atmospheric concentration of CO_2 at an acceptable level. The world reserve of fossil fuels is large and introduction of renewable energy sources are most likely not enough to achieve such a level of CO_2 during the next decades. One method to achieve CO_2-free combustion and still use fossil fuels as an energy source is to separate and dispose of the CO_2 from combustion (Lyngfelt and Leckner, 1999). Disposal costs are generally low, but a drawback with most methods is the decrease in efficiency and costly equipment necessary (Göttlicher *et al.*, 1998; Undrum *et al*., 2001). In chemical looping combustion (CLC) the separation of CO_2 is inherent and both reduced efficiency and separation costs can be avoided.

Chemical-Looping Combustion

In chemical looping combustion metal oxide particles are used to transfer oxygen from air to a gaseous fuel. The system consists of two separate reactors, as shown in Figure 1. In the fuel reactor the particles react with the fuel:

$$(2n+m)Me_xO_y + C_nH_{2m} \rightarrow (2n+m)Me_xO_{y-1} + mH_2O + nCO_2 \quad (1)$$

The reduced metal oxide is then transported to the air reactor where oxygen from the air is transferred to the particles:

$$Me_xO_{y-1} + ½O_2 \rightarrow Me_xO_y \quad (2)$$

*Corresponding author, e-mail address evjo@entek.chalmers.se

Thus, the reduced metal oxide is oxidized back to the original metal oxide and can be returned to the fuel reactor for a new cycle. Possible metal oxides are some oxides of common transition-state metals, such as iron, nickel, copper and manganese (Mattisson *et al.*, 2001a,b). For these oxides, reaction (2) is exothermic with subsequent heat release, while reaction (1) is most often endothermic. However, the total heat produced in the oxidation and the reduction is the same as in normal combustion where oxygen and fuel are in direct contact. The advantage with performing the combustion in two reactors/steps compared to conventional combustion is that the carbon dioxide is not diluted with nitrogen gas, but is received almost pure, without any extra energy demand and costly external equipment for CO_2 separation.

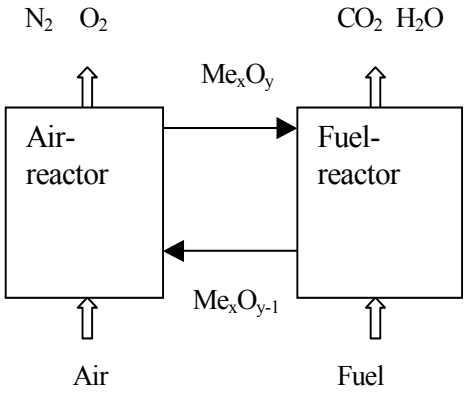

Figure 1. Chemical looping combustion (CLC). Me_xO_y and Me_xO_{y-1} denote oxidized and reduced oxygen carriers.

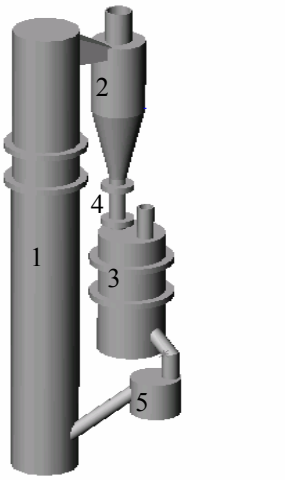

Figure 2. Layout of the model.1) air reactor, 2) cyclone, 3)fuel reactor, 4) downcomer 5) particle loop-seal

Different types of interconnected fluidized beds have been investigated by several authors, (*e.g.* Janse *et al.*, 1999 and Snip *et al.*, 1996). The CLC-system in Figure 2 is a circulating fluidized-bed system in which the air reactor (1), is the riser. The riser is connected by a cyclone (2) to the fuel reactor (3) in the form of a bubbling fluidized bed. Particle loop-seals, one in position (5) and one in the bottom of the downcomer from the cyclone, prevent gas mixing between the two reactors. In the process of developing a CLC-system, possible combinations of mass of oxygen carrier in the reactors, flow of oxygen carrier (external solids flux), air and fuel flows are crucial. First estimates of required external solids flux, G_s, under atmospheric conditions (Lyngfelt *et al.*, 2001) yield values of G_s in the order of 50 kg/m^{2}s, somewhat higher than for a typical large-scale conventional CFB combustor, (*e.g.* Zhang *et al.*, 1995). The tentative design by Lyngfelt *et al.* uses natural gas, iron oxide as oxygen carrier and has a thermal power of 10 MW. In the present work a similar design is used, but with the important difference that the system is pressurized to 0.9 MPa. The thermal power is 30 MW, the air ratio is 2.6 and the fluidization velocity is 3.5 m/s in the riser. Important aspects on the layout of the system are:

- The amount of oxygen carrier in the two reactors has to be adequate for sufficient conversion of reacting gas.
- The particle flow between the two reactors has to be high enough to transfer a sufficient amount of oxygen between the two reactors.
- Gas leakage between the reactors must be minimized.

The first two aspects are closely connected to the reaction properties of the oxygen carrier used. Several oxygen carriers with varying properties are under development, which means that no definite statements of the needed amounts/flows can be made. Furthermore, data for particle reactivity under pressurized conditions are still lacking. An important difference with increased pressure, when compared to atmospheric, is that the recirculation flow needs to be larger per cross section area. In addition, the amount of bed material may need to be larger, depending on the pressure dependence of the reaction rates. The amount of bed material in the fuel reactor is largely determined by the height of the overflow exit. However it is crucial to determine the relationship between the net solids flux between the reactors, G_s, the bed mass in the riser and the velocity in the riser. This work maps the range of G_s for various fluidization velocities and bed masses in the CLC-design suggested.

Net Solids Flux

There are several works that have mapped possible combinations of fluidization velocities, riser pressure drop and external solids flux (*e.g.* Li and Kwauk, 1980; Takeutchi *et al.*, 1986; Lim *et al.*, 1995 and references therein). These studies were focused on fast-fluidized beds, which typically operate at solids fluxes and with solids properties strongly different from those used in combustor systems. For the latter systems, with low solids fluxes, there is little information. G_s depends on fluidization velocity, solid properties and exit geometry, as seen from most correlations available for prediction of G_s (e.g. Johnsson *et al.*, 1999).

For a specific unit geometry, the net solids flux can be estimated from the solids density at the exit of the riser, ρ_{exit},

$$G_s = \rho_{exit} \cdot (u - u_t) = -\frac{1}{g} \cdot \left(\frac{dp}{dh} \right) \cdot (u - u_t) \qquad (3)$$

where the terminal velocity, u_t, is normally based on the average particle size for practical reasons - solid samples from top of riser are not normally available. Thus, the usefulness of this expression depends on the solids segregation effect (actual value of u_t at top of riser), accuracy in pressure drop measurement in upper part of riser and the ratio of solids externally recirculated to that internally separated at top of riser (Zhang *et al*, 1995; Johnsson *et al.*, 1998). This work includes an investigation on the applicability of Equation (3).

Experiment

Scale Model

A cold model in perspex was built and operated according to the simplified scaling laws for fluid dynamics proposed by Glicksman *et al.*, (1993). The following dimensionless numbers are kept constant during scaling:

$$\frac{u_0^2}{g \cdot L}, \frac{\rho_s}{\rho_f}, \frac{u_0}{u_{mf}}, \frac{L_1}{L_2}, \frac{G_s}{\rho_s \cdot u_0}, \phi, \textit{Particle size distribution} \quad (4)$$

Table 1 summarizes the scaling of a 30 MW CLC pressurized system to the ambient system. The basis for the scaling of the model is the air reactor with an inner diameter of 0.19 m and a height of 1.9 m, using air as fluid. The dimensions of the fuel reactor are also scaled, 0.19 m ID and 0.5 m in height, but since the fluid in the real combustor is a gaseous fuel, the density ratio in Equation (4) is not possible to fulfil with air. A hydrocarbon fuel would also react to form CO_2 and water, causing a dramatic increase in the volume flow as the gas passes the bed. This can obviously not be simulated in a cold model. The cyclone is not scaled, but was designed for optimal separation, and is therefore larger than the scaled size. The cold model is equipped with 24 pressure transducers. Some transducers measure differential pressure between two pressure taps, whereas some measure the pressure difference from one tap to the atmospheric pressure. The taps are inclined at an angle of 45° to prevent blocking and they are connected to a three-way valve to facilitate purging.

Table 1. Data for 30 MW_{th} unit and model scaled according to Eq. (4)

			30 MW_{th} unit	**Scaled model**
Temperature	T	°C	1000	20
Pressure	P	Pa	$9 \cdot 10^5$	$1 \cdot 10^5$
Gas viscosity	μ	Pas	$48.8 \cdot 10^{-6}$	$1.81 \cdot 10^{-6}$
Gas density	ρ_g	kg/m^3	2.46	1.19
Bed geometry	L	m	L	L/10
Particle diameter	d_p	μm	300	150
Solids density	ρ_s	kg/m^3	5240	2600
Superficial velocity	u_0	m/s	u	$0.32 \cdot u$
Solids flux	G_s	kg/m^{2}s	G_s	$0.16 \cdot G_s$

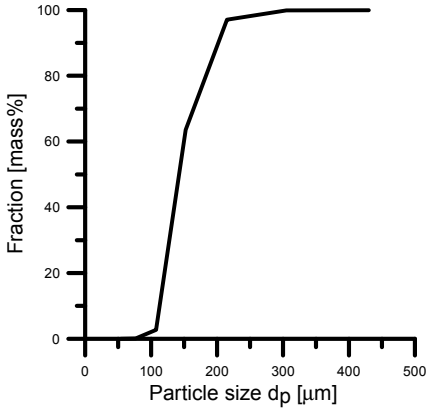

Figure 3. Particle size distribution of sand.

The particles are silica sand with a density of 2600 kg/m^3 and an average size of 0.15 mm. The size distribution is shown in Figure 3. A small amount of Larostat® powder No 519 was added to lower the static electricity. The fluidizing gas was air, and all experiments were conducted at room temperature. The air is added in the bottom through perforated plates serving as air distributors, and the number and dimensions of the holes are calculated according to Kunii and Levenspiel (1991). The gas flows to the reactors are controlled by rotameters.

The model was operated with different solids inventories in the range from 5 to 10 kg. The superficial gas velocity in the air reactor was varied from 0.7 to 1.2 m/s, while the velocity in the fuel reactor was held constant at 0.12 m/s in all runs. The latter corresponds to a flow that is somewhat lower than the product gas flow of CO_2 and H_2O. For the CLC design chosen this flow

has little effect on the fluid dynamics in the air reactor/riser. In order to obtain the solids hold-up and the vertical distribution of solids in the riser, the pressure drop was measured. The net solids flux, G_s, *i.e.* the circulation of material between the air and the fuel reactor, was measured by closing a butterfly valve in the downcomer, indicated by (4) in Figure 2.

Results

Figure 4 shows the pressure profiles in the riser for the lowest and highest mass in the system and lowest and highest velocities in the air reactor. The figure shows that the amount of bed material in the riser, which is given by the pressure drop, is reduced as the velocity increases. For the low velocity cases there is a dense bottom zone (strong gradient) in the lower part of the riser. Hence, there is a strong backmixing of solids in a splash zone above the dense zone.

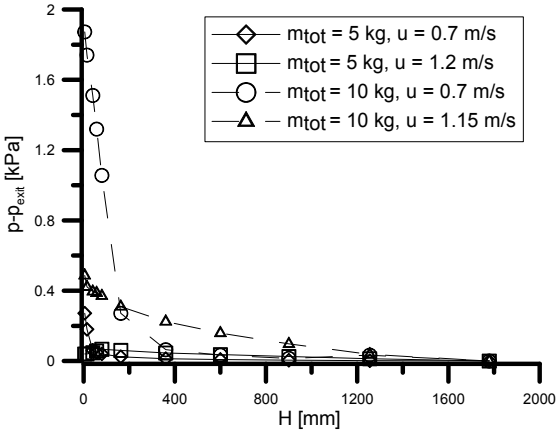

Figure 4. Pressure profiles in the air reactor.

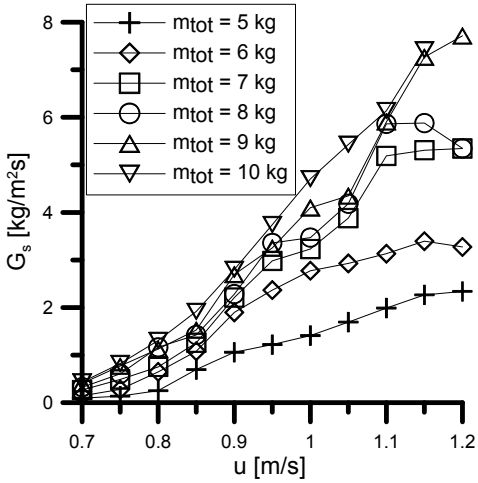

Figure 5. Average values of G_s versus superficial velocity in the air reactor.

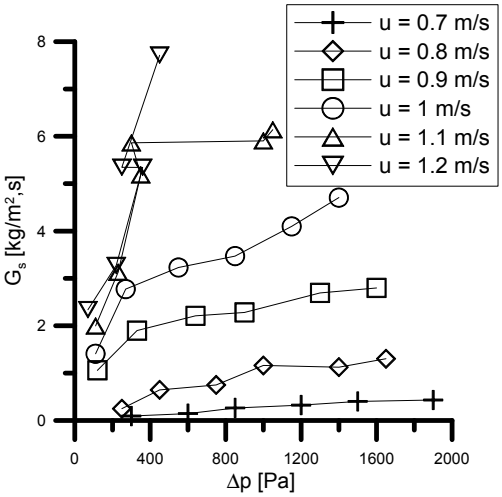

Figure 6. G_s as a function of the pressure drop for different superficial velocities.

Figure 5 shows the net solids flux of particles between the air and fuel reactor, G_s, as a function of the superficial velocity for the different solids inventories. All values are averages of six measurements, and there was a 20% relative scatter in these. As is evident from the figure, the net solids flux increases with increasing velocity as well as total mass. However, the increase in G_s is considerably lower for the two smaller masses, 5 and 6 kg, compared to the larger masses. For the lower masses, fulfilment of the pressure balance between the riser and the downcomer (cyclone side) at high

velocities results in that a dense bottom zone cannot be maintained in the riser. In these cases, solids back mixing in the riser is limited to occur in solids wall-layers. At high velocities for the series with 10 kg it was not possible to measure G_s at the velocity 1.2 m/s because the air reactor (riser) was depleted of solids, and the return system for the particles did not have enough capacity.

As can be seen from Figure 6, it is possible to cover a certain range of solids fluxes under constant superficial velocity in the air reactor, by changing the total solids inventory in the system (Figure 5). The maximum solids flux obtained is due to flow limitations in the downcomer section rather than that the maximum carrying capacity of the gas-solids suspension is reached. Figure 6 shows the variation in net solids flux (G_s) with the pressure drop of the air reactor (amount of solids) for different superficial velocities. For low velocities, G_s only increases slightly with the amount of solids in the air reactor, while for higher velocities, 1.1 and 1.2 m/s, the increase is much greater. The terminal velocity for the average particle size is 0.87 m/s and for low velocities only a small fraction of the solids is entrainable, which may explain the small increase in net solids flux. For high velocities, the velocity exceeds the terminal velocity of almost all solids and, thus, a much greater fraction of the sand is recirculated. For the highest velocities the conditions in the model are somewhat unstable, which explains the irregularities of the two curves 1.1 and 1.2 m/s.

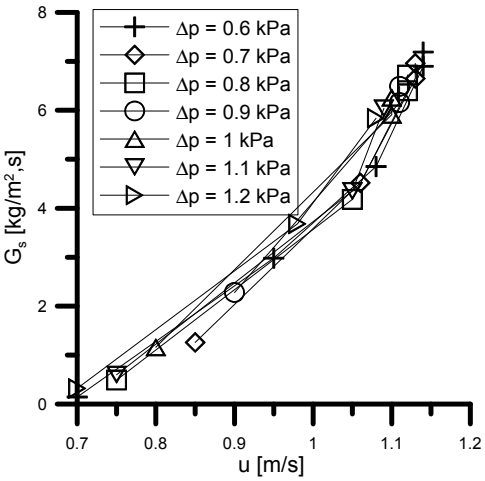

Figure 7. G_s versus velocity for different pressure drops

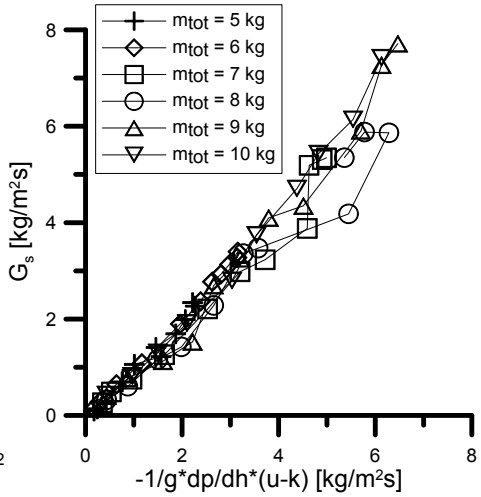

Figure 8. Measured G_s against Eq. (3) with k as a fitting parameter (k=0.25).

In Figure 7 the net solids flux from the air to the fuel reactor is shown as a function of the superficial velocity for different total pressure drops over the air reactor. The increase in net solids flux is rather independent of the pressure drops, or mass of solids, in the air reactor. The range of pressure drops included in Figure 7 corresponds to values for which G_s could be varied over a wide range. The total range of pressure drops investigated, however, is much larger, see Figure 6.

Figure 8 compares measured values of net solids flux with those estimated from Equation (3). The data fits Equation (3) if terminal velocity is used as a fitting parameter and set to 0.25. The reason why the terminal velocity of an average sized bed particle cannot be employed is due to the above-mentioned effects of solids

segregation, ratio of internal to external flux at top of riser and accuracy in pressure drop measurements. More detailed measurements are needed to separate the influence of these effects.

Discussion

The net solids flux measured in the present system ranged between 0.1 and 8 kg/m^{2}s, Figure 5, which corresponds to a net solids flux between 0.6 and 50 kg/m^{2}s in the pressurized combustor, Table 1. In a design calculation of an atmospheric CLC system, a suitable solids flux was estimated to 13 kg/sMW$_{th}$, (Lyngfelt *et al*. 2001). This value is based on iron oxide as oxygen carrier in an atmospheric boiler with only a 2% conversion difference of the oxide between the fuel and air reactor. The conversion difference indicates how much of the theoretical maximum change in conversion, *i.e.* between fully oxidized state and fully reduced state, is used when the particles are circulated (Lyngfelt *et al*., 2001). The conversion difference is inversely proportional to the required net solids flux. With a fluidization velocity of 1.11 m/s and G_s of 6 kg/m^{2}s, which corresponds to a fluidizing velocity of 3.5 m/s and a G_s of 38 kg/m^{2}s in the 30 MW$_{th}$ pressurized combustor, the oxygen carrier would need to have a conversion difference of about 7.5%.

It is not possible at present to safely predict whether the iron oxides under development will reach these conversions in practice, although results are promising, (Mattisson *et al.,* 2001a,b). If this would not be achieved either a higher net solids flux would be needed or the choice could be another oxygen carrier with higher capacity of oxygen transfer.

The pressure drop in the riser of 1 kPa in the scaled model corresponds to a pressure drop of 20 kPa in the full-scale unit, because of increased height and particle density. This gives a needed conversion rate of 8%/min. Laboratory data indicate that such conversion rates are realistic even at atmospheric pressure (Mattisson *et al.,* 2001a,b). Thus, the amount of bed material used in the present study is realistic.

Conclusions

A conceptual design of a pressurized CLC system was explored in order to map suitable conditions for the riser, to meet the object of achieving both a sufficient net solids flux between the reactors and an appropriate bed mass in the riser. From these data possible operating conditions are suggested. It should be pointed out that the possible operating conditions are closely dependent on the reaction properties of the oxygen carriers and may be reconsidered, as more data from the development of these will become available.

Notation

d_p	particle diameter [m]	u_0	superficial velocity [m/s]
g	acceleration due to gravity [m/s^2]	u_{mf}	minimum fluidization velocity [m/s]
G_s	net solids flux [kg/m^{2}s]	u_t	terminal velocity [m/s]
h	height [m]	Δp	pressure drop [Pa]
k	u_t fitting parameter in Eq. (3) [m/s]	p	pressure [Pa]
L	length [m]	T	temperature [K]

ϕ	particle coefficient	ρ_f	density of the fluid [kg/m^3]
μ	dynamic viscosity [Pas]	ρ_s	density of the solids [kg/m^3]
ρ_{exit}	density in the exit of the riser [kg/m^3]		

References

Glicksman, L.R., M. Hyre and K. Knowlton, "Simplified Scaling Relationships for Fluidized Beds", Powder Tech. **77**, 177-199, (1993)

Göttlicher, G., and R. Pruschek, "Analysis of Development Potentials for Power Stations with CO_2 Removal/Concentration" in " Proceedings of the 4th Int. Conf. on Greenhouse Gas Control Technologies", Interlaken (1998), pp 83-88

Janse, A.M.C., P.M. Biesheuvel, W. Prins, W.P.M. van Swaaij, "A Novel Interconnected Fluidised Bed for the Combined Flash Pyrolysis of Biomass and Combustion of Char", Chem. Eng. J. **75**, 121-130, (1999)

Johnsson, F., C. Breitholtz and B. Leckner, "Solids Segregation in a CFB-Boiler Furnace", in "Fluidization IX", L-S. Fan and T. Knowlton, Eds., Engineering Foundation (1998), pp. 757-764

Johnsson, F., A. Vrager and B. Leckner, "Solids Flow Pattern in the Exit Region of a CFB-Furnace - Influence of Exit Geometry" in "Proc. 15th Int. Conference on Fluidized Bed Combustion", Savannah, (1999)

Kunii, D. and O. Levenspiel, "Fluidization Engineering", Reed publishing Inc., Stoneham (1991)

Li, Y. and M. Kwauk, "The Dynamics of Fast Fluidization" in "Fluidization", J. R. Grace and J. M. Matsen, Eds. Plenum Press, New York, (1980), pp 537-544

Lim K. S., J. X. Zhu and J. R. Grace, "Hydrodynamics of Gas-Solid Fluidization", Int. J. Multiphase Flow, **21**, 141-193, (1995)

Lyngfelt, A. and B. Leckner, "Technologies for CO_2 Separation", in "Minisymposium on Carbon Dioxide Capture and Storage", A. Lyngfelt and C. Azar, Eds., School of Environmental Science, Chalmers University of Technology and Göteborg University, Göteborg (1999), pp 25-35, http://www.entek.chalmers.se/~anly/symp/sympco2.html

Lyngfelt, A., B. Leckner and T. Mattisson, "A Fluidized-Bed Combustion Process with Inherent CO_2 Separation; Application of Chemical-Looping Combustion", Chem. Eng. Sci. **56**, 1-13, (2001)

Mattisson, T., A. Lyngfelt, and P. Cho, "The Use of Iron Oxide as an Oxygen Carrier in Chemical-Looping Combustion of Methane with Inherent Separation of CO_2", Fuel **80**, 1953-1962, (2001)

Mattisson, T., A. Lyngfelt and P. Cho, "Possibility of Using Iron Oxide as an Oxygen Carrier for Combustion of Methane with Removal of CO_2 - Application of Chemical-Looping Combustion", in "Proceedings of the 5th Int. Conf. of Greenhouse Gas Control Technologies", D.J. Williams, *et al*., Eds., CSIRO publishing, Cairns, Australia (2001), pp. 205-210

Snip, O.C., M. Woods, R. Korbee, J.C. Schouten, C.M. van den Bleek, "Regenerative Removal of SO_2 and NO_x for a 150 MWe Power Plant in an Interconnected Fluidized Bed Facility", Chem. Eng. Sci. **51**, 2021-2029, (1996)

Takeuchi, H., T. Hirama, T. Chiba, J. Biswas and L. S. Leung, "A Quantative Regime Diagram for Fast Fluidization", Powder Tech. **47**, 195-199, (1986)

Undrum, H., O. Bolland and E. Aarebrot, "Economical Assessment of Natural Gas Fired Combined Cycle Power Plant with CO_2 Capture and Sequestration", in "Proceedings of the 5th Int. Conf. of Greenhouse Gas Control Technologies", D.J. Williams, *et al*., Eds., CSIRO publishing, Cairns, Australia (2001) pp. 167-172

Zhang, W., F. Johnsson and B. Leckner, "Fluid-Dynamic Boundary Layers in CFB Boilers", Chem. Eng. Sci. **50** 2, 201-210 (1995)